Current-Mode High-Precision Full-Wave Rectifier Based on Carbon Nanotube Field Effect Transistors

Neda Talebipour[1], Peiman Keshavarzian[2]
1- Young Researchers and Elite Club, Kerman Branch, Islamic Azad University, Kerman, Iran
Email: n.talebipour@iauk.ac.ir (Corresponding author)
2- Department of Computer Engineering, Kerman Branch, Islamic Azad University, Kerman, Iran
Email: keshavarzian@iauk.ac.ir

Received: June 2014 Revised: March 2015 Accepted: May 2015

ABSTRACT:
This paper presents a novel design of a high performance current mode (CM) precision full-wave rectifier by using just four diode-tied carbon nanotube field effect transistors. To compare the behavior of the proposed design, the frequency dependent RMS error and DC transient value for different values of input current amplitudes are evaluated. Extensive simulation results using HSpice demonstrate that the proposed circuit has a good performance at high frequencies. The main advantages of the proposed design over the previous designs are the minimal number of the transistors, small size, circuit simplicity, high accuracy and capability of rectifying low-level signals at high frequencies with little or no distortion. The circuit also provides good temperature stability.

KEYWORDS: Carbon Nanotube Field Effect Transistors, Current Mode, Precision Full-Wave Rectifier.

1. INTRODUCTION

Full-wave rectifier circuits have various applications in analog electronics such as AC measurements, function fitting, providing inputs to single-quadrant devices, triangular-wave frequency doubling, error measurements, average envelope detection and clock recovery [1, 2]. Generally, diodes are used for rectification, but sometimes, we need to rectify a signal with an amplitude less than the threshold voltage of the diode [3]. By combining diodes with operational amplifiers, one can overcome the diode threshold voltage, and obtain rectifier circuits with precise characteristics, thus these circuits can rectify the low-level signals. However, such circuits can only have a good performance at low frequencies, while they cause average or severe distortions at frequencies almost more than 1 KHz [4].

Various rectifier circuit designs have been proposed by many researchers [35-47].Implementation of the most rectifier designs [35-47] has been done by conventional MOSFET technology. Nowadays because of the limitation of traditional silicon transistors, it is gradually replaced by new technologies and devices that are the achievement of nanotechnology such as quantum-dot cellular automata (QCA), spin-wave architecture, single electron devices, quantum computing and carbon nanotube field effect transistor (CNTFET). As we progress into an era of nanotechnology, molecular devices are becoming promising alternatives to the existing silicon technology. Nanotechnology is a new field of research that cuts across many fields – electronics, chemistry, physics, and biology, that analyzes and synthesises objects and structures in the nano scale (10^{-9} m) such as nano particles, nanowires and carbon nanotubes (CNTs). CNT is one of the several cutting-edge emerging technologies within nanotechnology with high efficiency and a wide range of applications in many different streams of science and technology. Nanocircuits based on CNTs such as CNT field effect transistors (CNTFETs) show big promise of less delay and power consumption than available silicon-based FETs. Carbon nanotube has attracted attention in recent years not only for its relatively small dimensions and unique morphologies but also for its potential of implementation in many current and emerging technologies. CNT is made up of graphite. It has been observed that graphite can be formed in nano-scale in three forms: (1) carbon nano ball (CNB) (or Bucky ball) (2) carbon nanotube (CNT) that comes mainly in two types: (a) multi-wall CNT (MWCNT), and (b) single-wall CNT (SWCNT), and (3) carbon nano coil (CNC). Many studies and circuit designs through CNTFET have been proposed by CNTFET researchers [21-34].

For a number of years, current mode circuits have been recognized as the main opponent of the voltage mode circuits. Current-mode (CM) compared to voltage-mode (VM) has numerous advantages among which are higher usable gain, greater linearity, lower power consumption, wider bandwidth, lower number of components and larger dynamic range [5] . Since current mode circuits have better performance at high frequencies, a lot of rectifications have been designed in this mode. The rectifier circuit suggested by Kumngern [3] has a very low precision. This circuit rectifies an input current with amplitude of 20 µA and frequency of 300 MHZ with a high voltage drop. In this design, numerous transistors have also been employed. Koton [6] has also used a number of transistors to design rectifier circuits. This circuit rectifies a signal with amplitude of 5 µA and frequency of 1 MHz with a considerable distortion. Moreover, the cut-off frequency of this circuit for an input current with amplitude of 5 µA is 15 MHz. However, for the mentioned input, the cut-off frequency of the proposed circuit is 140 GHz which is capable of rectifying the current with little or no distortion at frequencies less than 10 GHz. The performance of the proposed circuit at high frequencies is far better than the full wave rectifier based on 2 diodes and a CDTA structure which proposed in [7].The cut-off frequency of our proposed design for an input current with amplitude of 10 µA is 190 GHz, while for this input current, the cut-off frequency of their proposed circuit [7] is almost 4.9 MHz. In this article, only four Carbon nanotube field effect transistors were used to implement the full-wave rectifier. The threshold voltage of CNTFET can be adjusted by changing the chirality vector [8]. In this paper this feature is used to implement high precision rectifier. The simulation results demonstrate that our proposed design have better performance in comparison to the previous work.

The remaining of this paper is organized as follows. Section 2 shows the review of CNTFETs. Section 3 presents our design of a new rectifier. Section 4 includes simulation results, and finally in section 5 conclusion is presented.

2. REVIEW OF CNTFETS

Carbon nanotube field effect transistor is a propitious technology which has been replaced with primitive silicon devices. A field-effect transistor (FET) was successfully fabricated based on a single wall carbon nanotube (SWCNT) and proved to be able to operate at room temperature in 1991 [9]. Carbon nanotube field-effect transistors (CNTFETs) have attracted a lot of attention as the next-generation devices in Nano Electronics. Figure 1(a) illustrates a one-dimensional conductor named single walled carbon nanotube (SWCNT) which can be either metallic or semiconducting depending on the arrangement of carbon atoms defined by their Chirality, Ch (i.e. the direction in which the graphite sheet is rolled) whose magnitude with CNT diameter (DCNT) is given by (1) and (2) respectively, and where ‘a’ is the graphite lattice constant (0.249nm), and n1 and n2 are positive integers that specify the chirality of the tubes. SWCNT can be imagined as a sheet of graphite which is rolled up and joined together along a wrapping vector (1), as shown in Figure 1(b), where a1 and a2 are unit vectors [10]. The CNT is called zigzag if n1= 0, armchair if n1= n2, otherwise nanotube will be chiral.

$$C_{\mathrm{h}} = \sqrt{n_1.a_1 + n_2.a_2} \quad (1)$$

$$D_{\mathrm{cnt}} = C_h / \pi \quad (2)$$

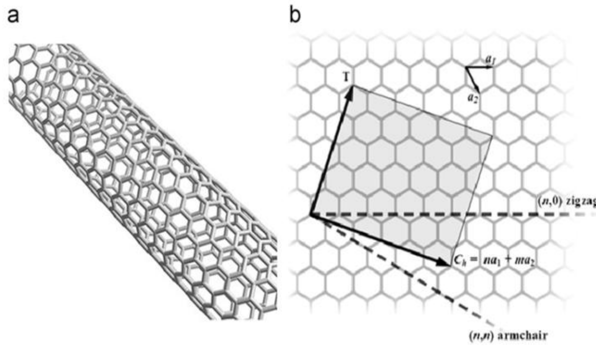

Fig. 1. (a) SWCNT (b) Graphite sheet in terms of chirality n1 and n2

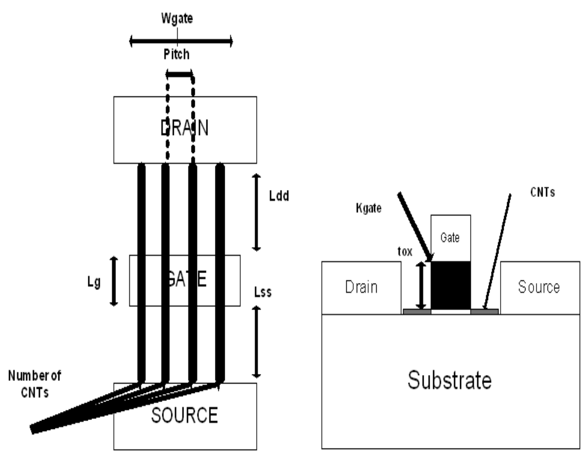

Fig. 2. Schematic CNFET cross-section

Substituting a number of semiconducting carbon nanotubes for the channel of a conventional MOSFET is one of the particular details of CNTFET as shown cross-section in Figure 2 [11]. The operation principle of CNTFET is the same as traditional MOSFET. Since electrons are only limited to a narrow nanotube, the mobility rises substantially due to the ballistic transport as compared with the bulk MOSFET [12]. There are two types of carbon-nanotube transistors that are extensively studied .One is a tunnelling device (Figure 3(a)), that works on the principle of direct tunnelling through a Schottky barrier at the source–channel junction. The barrier width is modulated by using gate voltage so that the transconductance of the device is dependent on the gate voltage [13]. To overcome these disadvantages associated with Schottky barrier CNTFETs, there have been some attempts to develop CNTFETs so that they behave like normal MOSFETs. Being potentially noticeable, these attempts have been significantly successful. The MOSFET-like CNTFET (Figure 3(b)) operates on the principle of barrier height modulation by using gate potential. In this paper, we will consider a non-Schottky-barrier MOSFET-like unipolar CNTFET with ballistic transport as our device of interest.

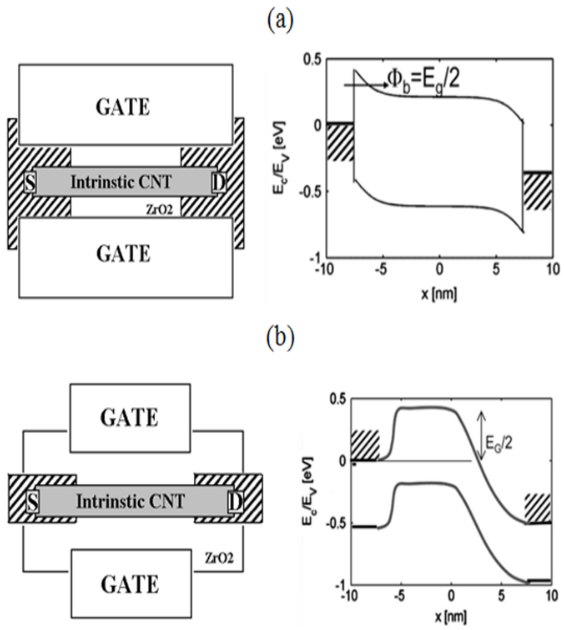

Fig. 3. Two types of single walled CNTFETs.

Hereafter in this paper the abbreviation CNTFET will be used to denote a MOSFET-like device unless stated otherwise. Figure 3(b) shows the band diagram of this device [13-15]. The source Fermi level for a degenerately doped source can be derived from the conduction band edge. Inside the intrinsic channel, the Fermi level is in the middle of the band-gap. An important property of these CNTFETs is that the band-gap is in inverse correlation with the diameter of the nanotube as in (3) [16, 17]. As the barrier height determines the threshold potential of a FET, the threshold voltage of the CNTFETs can be expressed as in (4).

$$E_g = \frac{0.84}{d(nm)} ev \qquad (3)$$

$$V_{th} \approx \frac{E_g}{2e} = \frac{\sqrt{3}}{3}\frac{aV_\pi}{eD_{CNT}} \qquad (4)$$

DCNT is the CNT diameter, e is the unit electron charge, Vπ=3.033 eV is the carbon π–π bond energy in the tight bonding model, and a=2.49 Å is the carbon-to-carbon atom distance. For example, the threshold voltage of the CNTFETs that use (19, 0) CNTs as channels is 0.289 V because the DCNT of a (19, 0) CNT is 1.49 nm. Simulation results have acknowledged the validity of this threshold voltage. Since the vector changes, the CNTFET thresh-old voltage will also change. The threshold voltage of the CNTFET is inversely related to the CNT chirality vector. The threshold voltage of the CNTFET using (13, 0) CNTs is 0.423 V, whereas the threshold voltage of the CNTFET by means of (19, 0) is 0.289 V. Figure 4 shows the threshold voltage of both P- and N-type CNTFETs obtained from (2) and HSPICE simulation results for various chirality vectors (various n1 for n2=0). The current–voltage (I–V) characteristic of the CNTFET with different gate lengths is shown in Figure 4, which shows that the I–V characteristics of the CNTFET are similar to those of the MOSFET. The CNTFET circuit current is saturated at higher Vds (drain to source voltage) as the channel length increases, as shown in Figure 5. The energy quantization in the axial direction at a 32-nm (or less) gate length causes the on-current to decrease, as expected [19].

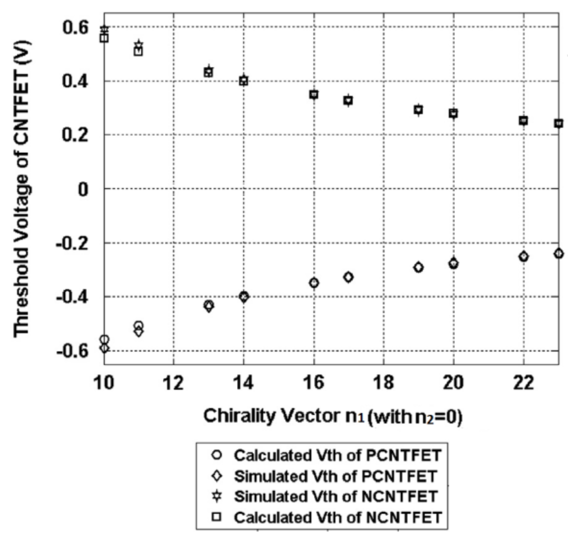

Fig. 4. Threshold voltage of the CNTFETs versus n1 (for n2 = 0).

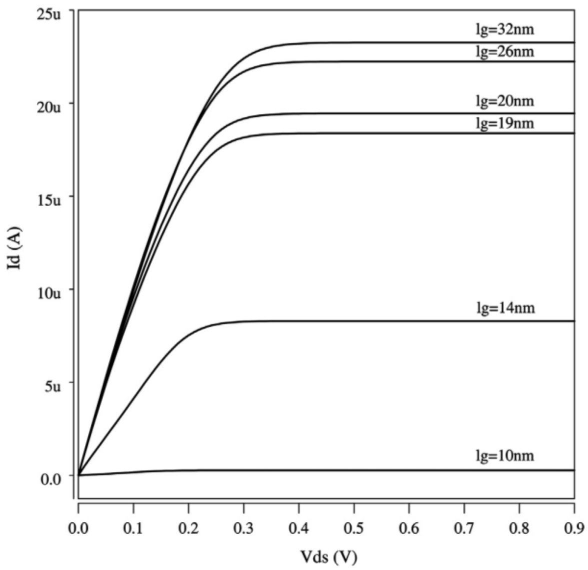

Fig. 5. Current-voltage (I-V) characteristics of a ballistic CNTFET

3. PROPOSED DESIGN

This design consists of just four N-type carbon nanotube field effect transistors (Figure 6). By connecting gate and drain in M1, M2, M3 and M4 transistors, these transistors will operate as a diode (By connecting gate and drain in carbon nanotube field effect transistor, this device can be easily converted into a diode, similar to diode-connected transistor in silicon device [18].) , thus if the gate voltage is greater than the source voltage, the diode-connected transistors will pass the current, and if gate voltage is less than the source voltage, these transistors will be turned off. The operation of proposed circuit is as follows: When input current is positive, since gate and drain in M1 and M2 are connected to the earth and also according to the input current direction, the gate voltage in M1 becomes less than the source voltage, and in M2 the gate voltage becomes greater than the source voltage, therefore M1 will be switched off, and M2 will be turned on. Meanwhile, M3 and M4 will be turned on and off respectively (according to the transistors type and input current direction). As a result, input current will flow through M3 to the output, and therefore Ioutput will become equal to Iinput. Similarly, when Iinput is negative, since in M1 and M4 gate voltage is greater than the source voltage, these diodes-connect transistors will be turned on, and M2 and M3 will also be turned off because gate-source voltage in these transistors is negative. As a result, "-I input" will flow through M4 to the output. Thus, Ioutput will be always positive. To simulate our circuit design, we used the STANFORD compact model of CNTFETS [19]. The values of Lch, Lgeff, Lss, Ldd and Efi parameters which are used in this model are 32nm, 100nm, 32nm, 32nm and 0.6EV, respectively, where Lch and Lgeff represent physical channel, and mean free path in intrinsic CNT channel; also Lss, Ldd and Efi mean the length of doped CNT source side extension region, length of doped CNT drain-side extension region and Fermi level of the doped S/D tube. The values of Kgate, Tox, Csub, Csd and Pitch are 16, 4nm, 20PF/M, 0 pF/m, 20nm respectively where Kgate and Tox show dielectric constant of high-k top gate dielectric material and thickness of high-k front gate dielectric material. Csub is the coupling capacitance between channel region and substrate; Csd is the coupling capacitance between channel region and source/drain region, and Pitch is the distance between the center of two adjacent tubes under the same gate. n1, n2 in this model represents the chirality of tube, and their values are 29 and 0, respectively.

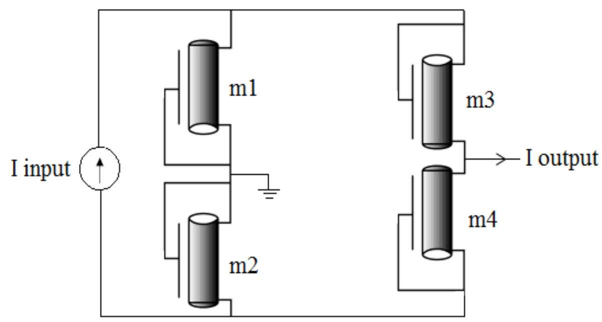

Fig. 6. The proposed Precision Full-Wave Rectifier.

4. SIMULATION RESULTS

In this article we use CNT field effect transistors to implement our circuit designs. In order to observe the transient behavior of the circuits and to verify the functionality of our rectifier, simulations have been done by means of HSpice simulation tool. We apply the SPICE model from [19] which is described in more detail in [16] and [17].

Figure 7 shows the DC transfer characteristic, which confirms precise rectification over a range of input currents [-108uA, 108uA].

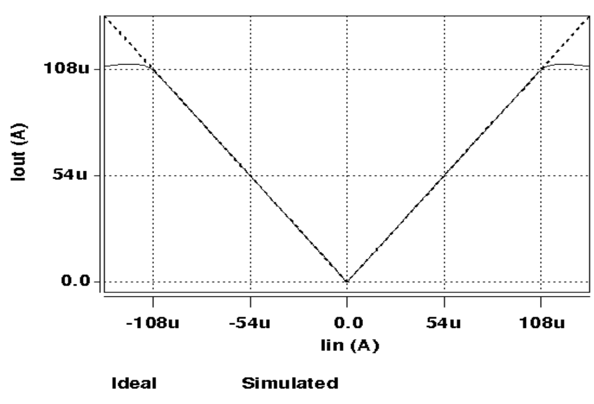

Fig. 7. DC transfer characteristic of proposed circuit

To evaluate the behavior of the proposed circuit at different frequencies and amplitudes of input signal, the DC value transfer (PDC) and RMS error (PRMS) have been analyzed [20]:

$$P_{DC} = \frac{\int_T y_R(t)d(t)}{\int_T y_{ID}(t)d(t)} \quad (5)$$

$$P_{RMS} = \sqrt{\frac{\int_T [y_R(t) - y_{ID}(t)]^2 dt}{\int_T y_{ID}^2(t)dt}} \quad (6)$$

Where T is the period of the input signal, and YR (t) and YID (t) represent the actual and ideal output signal. For ideal rectifier, i.e. where YR (t) = YID (t), the DC value transfer and root mean square error are equal to "1" and "0", respectively. Figure 8 shows the PDC (a) and PRMS (b) for input signal magnitudes of 0.1µA, 5µA and 10µA in various frequencies (10 MHz to 1 THz).

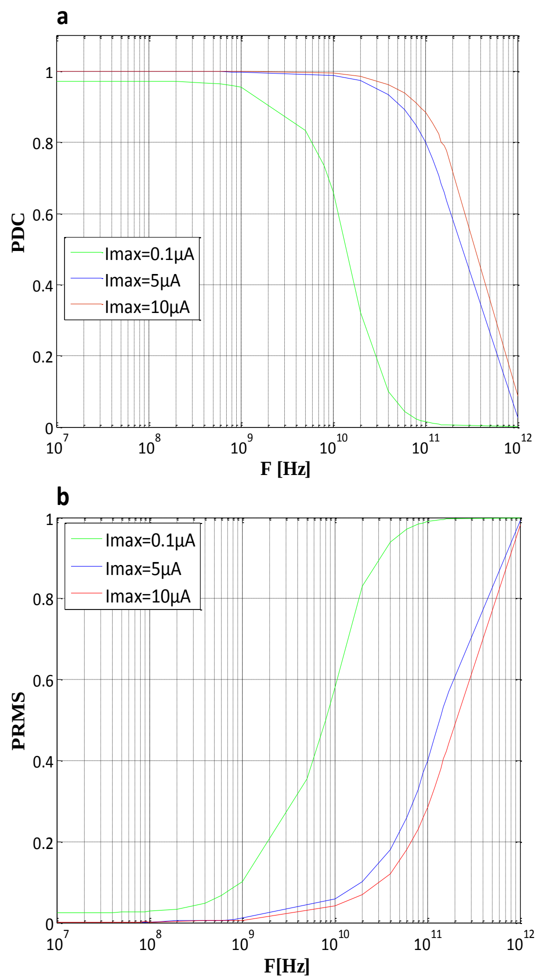

Fig. 8. (a) DC value transfers, (b) RMS errors for input signal amplitudes 0.1 µA, 5 µA, and 10 µA

Increasing the frequency and/or decreasing the amplitudes of the input signal causes distortion, and the PDC value decreases to less than the ideal value; PRMS also increases above the zero value. As can be observed in Figure 8, the -3db cutoff frequency of DC value transfer for the input current magnitude of 0.1µ, 5µ and 10µ is about 9GHz, 140GHz, and 190GHz respectively. The transient responses for frequencies of 100 MHz, 1 GHz, 10 GHz, 40 GHz and an input signal amplitude of 10µ are shown in Figure 9. The proposed circuit is able to rectify 100 MHz input signal without any distortion (Figure 9a). A little distortion of the output signal, mainly in the zero crossing area, appears with 1 GHz and 10 GHz input signal (Figure 9b and Figure 9c). This distortion increases with increasing the frequency of the input signal (for 40 GHz input signal significant distortion can be observed (Figure 9d)) , which is in agreement with the decreasing value of PDC to less than the ideal unity value (Figure 8a) and/or increasing the value of PRMS above the zero value (Figure 8b).

Simulation results of rectifiers for input signal amplitudes 5 µA, 20 µA, and 50 µA are shown in Table 1. It demonstrates that our proposed design has the best results than the state-of-the-art rectifier circuit design [6].

Table 1. Simulation results of the rectifiers for input signal amplitudes 5 µA, 20 µA, and 50 µA

input signal amplitude	**Design**	**Technology**	**-3 dB Cutoff frequency**
5 µA	Proposed	CNTFET Lg=32nm	140 GHz
	Based on [6]	CMOS Lg=32nm	15 MHz
20 µA	Proposed	CNTFET Lg=32nm	326 GHz
	Based on [6]	CNTFET Lg=32nm	27 MHz
50 µA	Proposed	CMOS Lg=32nm	467 GHz
	Based on [6]	CMOS Lg=32nm	50 MHz

Figure 10 shows the transient response of the output waveforms for input signal of 100 MHz and amplitudes from 1 µA to 101 µA with step of 25 µA. It is obvious here that the rectifier is capable to rectify a wide range of amplitudes.

Temperature analysis of the DC transfer characteristic with temperature in range of 0–100 °C were provided, and the simulation shows an overlapped curves confirming a good temperatures stability of the proposed circuit (Figure 11).

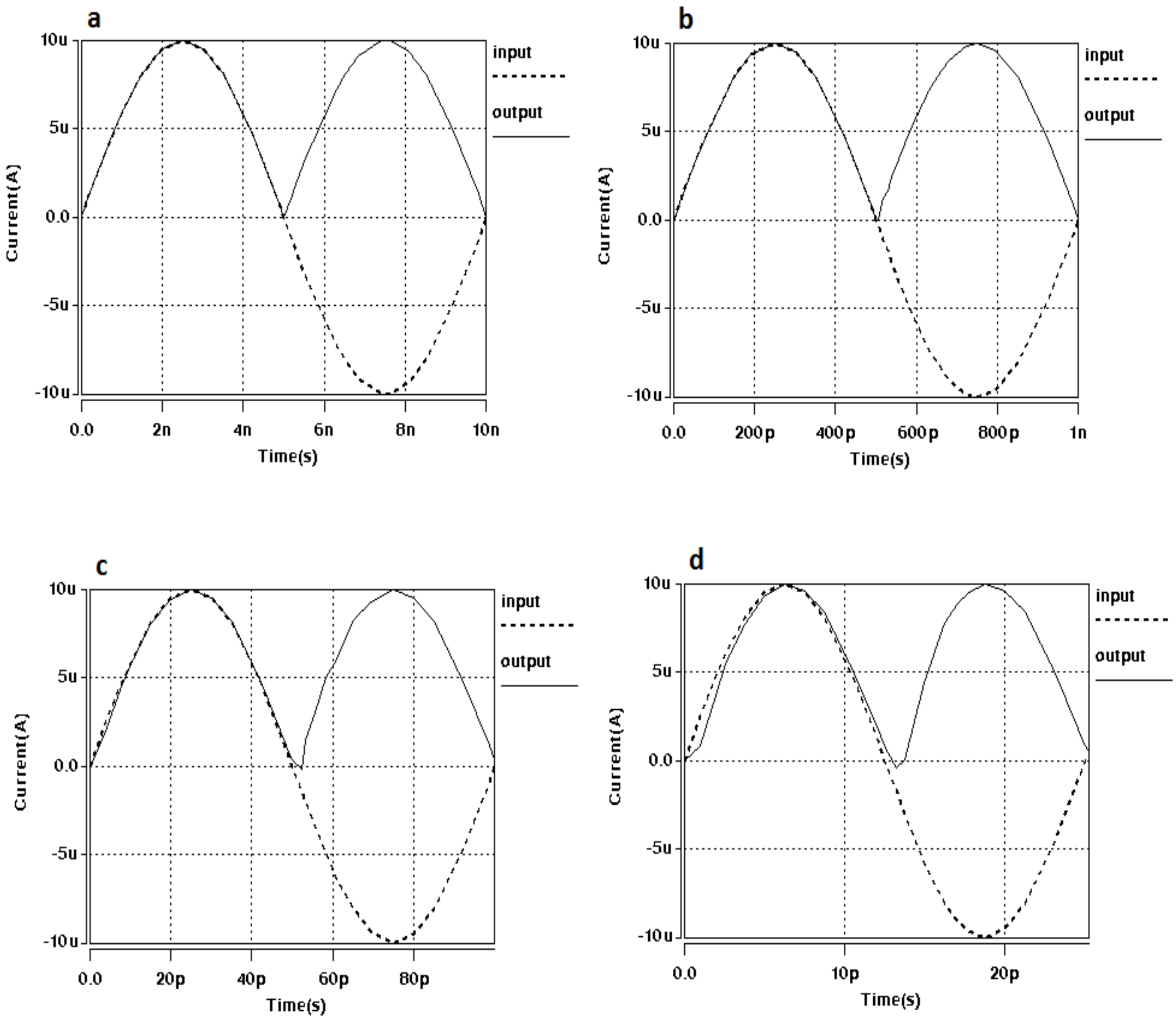

Fig. 9. Transient responses of the proposed design for input signal amplitude 10µA (a) f=100 MHz (b) f=1 GHz (c) f=10 GHz (d) f=40 GHz

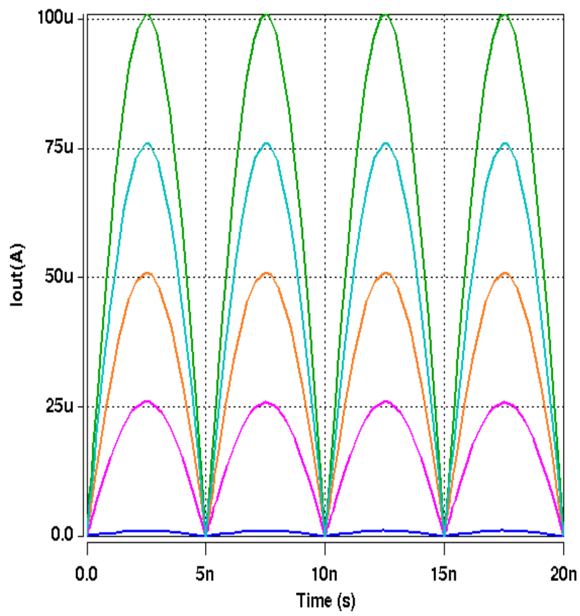

Fig. 10. Transient analyses of the output waveforms with 100 MHz and various amplitudes of the input signal

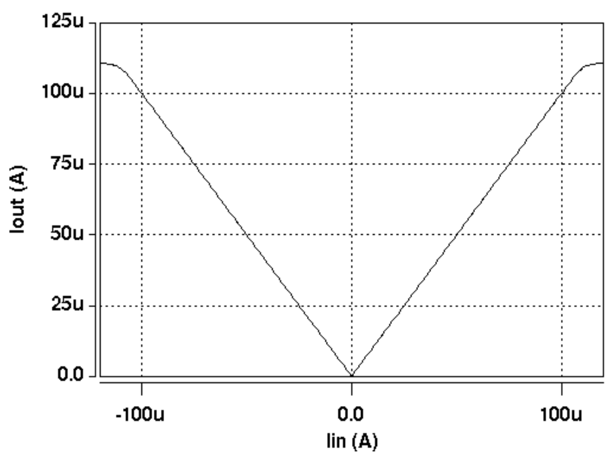

Fig. 11. DC transfer characteristic of the proposed full-wave rectifier at different temperatures

5. CONCLUSION

A design of high precision rectifier circuit has been proposed in this paper. This design consists of just four diode-tied carbon nanotube field effect transistors. The main attractive features of the proposed design are minimal number of transistors, small size, circuit simplicity, high accuracy and capability of rectifying signals with a relatively wide range of frequencies and amplitudes. The performance of the rectifier was analyzed by evaluating the frequency dependent RMS error and DC transient value for different values of input current magnitudes. The simulation results using HSPICE demonstrate that the -3db cutoff frequency for the input current magnitude of 0.1µA, 5µA, 10µA, 20µA, 50µA is about 9GHz, 140GHz, 190GHz, 326GHz and 427GHz, respectively. Simulation results of various temperatures (0°C–100°C) show that the proposed rectifier provides good temperature stability.

REFERENCES

[1] P. Sahu, M. Singh, and A. Baishya, **"A novel versatile precision full-wave rectifier, "** *IEEE Transactions on Instrumentation and Measurement*, Vol. 59, No. 10, pp. 2742-2746, October. 2010.

[2] A. A. Ciubotaru, **"Absolute-value circuit using junction field-effect transistors,"** *IEEE Transactions on Circuits and Systems—II: Analog and Digital Signal Processing*, Vol. 50, No. 8, pp. 481-484, August 2003.

[3] M. Kumngern, **"Cmos current-mode precision full-wave rectifier with improved bandwidth,"** Digital Information and Communication Technology and it's Applications (DICTAP), Second International Conference on. Bangkok, pp. 283 – 286, May. 2012.

[4] C. Toumazou and F. J. Lidgey, **"Fast current-mode precision rectifier,"** *Electron. Wireless World*, Vol. 93, No. 1621, pp. 1115–1118, 1987.

[5] SH. Minaei and E. Yuce, **"New squarer circuits and a current-mode full-wave rectifier topology suitable for Integration,"** *Radioengineering*, Vol. 19, No. 4, pp. 657 – 661, December. 2010.

[6] J. Koton, A. Lahiri, N. herencsar and K. Vrba, **"Current-Mode Dual-Phase Precision Full-Wave Rectifier Using Current-Mode Two-CellWinner-Takes-All (WTA) Circuit,"** *Radioengineering*, Vol. 20, No. 2, pp. 428-432, June. 2011.

[7] F. KHateb, J. Vavra and D. Biolek, **"A Novel Current-Mode Full-Wave Rectifier Based on One CDTA and Two Diodes,"** *Radioengineering*, Vol. 19, pp. No. 3, pp. 437-445, September 2010.

[8] SH. Lin, Y. Kim, F. Lombardi, **"Design of a ternary memory cell using CNTFETs",** *IEEE Transactions on Nanotechnology***,** Vol. 11, No. 5, pp. 1019 – 1025, September. 2012.

[9] S. Iijima, **"Helical microtubules of graphic carbon,"** *Nature*, 345, pp. 56–58, November. 1991.

[10] S. J. Tans, A. R. M. Verschueren and C. Dekker, **"Room- temperature transistor based on a single carbon nanotube,"** *Nature*, Vol. 393, pp. 49 – 59, May. 1998.

[11] P. L. Mceuen, M. S., Fuhrer and H. Park, **"Single-walled carbon nanotube electronics,"** *IEEE Tran on Nanotechnology*, Vol. 1, No. 1, pp. 78 – 85, March. 2002.

[12] P. Avouris, J. Appenzeller, R. Matrel and S. J. Wind, **"Carbon nanotube electronics,"** *Proceeding of IEEE*, Vol. 91, No. 11, pp. 1772 – 1784, November. 2004.

[13] J. S. Hwang, H. T. Kim, M. H. Son, J. H. Oh, S. W. Hwang and D. Ahn, **"Electronic transport properties of a single-wall carbon nanotube field effect transistor with deoxyribonucleic acid conjugation,"** *Physica E: Low-dimensional Systems and Nanostructures*, Vol. 40, No. 5, pp. 1115 – 1117, March. 2008.

[14] M. Pourfath, ET AL**, "Numerical Analysis of Coaxial Double Gate Schottky Barrier Carbon Nanotube Field Effect Transistors,"** *Journal of Computational Electronics*, Vol. 4, No. 5, pp. 75 – 78, 2005.

[15] J. Guo, A. Javey, H. Dai, S. Datta and M. Lundstrom, **"Predicted Performance advantages of carbon nanotube transistors with doped nanotubes source/drain,"** *Phys Rev B Condens.Matter,cond-mat/0 309 039*, 2003.

[16] J. Deng, H. S. P. Wong, **"A Compact SPICE Model for Carbon-Nanotube Field-Effect Transistors Including Nonidealities and Its Application - Part I: Model of the Intrinsic Channel Region,"** *IEEE Trans Electron Devices*, Vol. 54, pp. 3186-3194, December. 2007.

[17] J. Deng, H. S. P. Wong, **"A Compact SPICE Model for Carbon-Nanotube Field-Effect Transistors Including Nonidealities and Its Application - Part II: Full Device Model and Circuit Performan Benchmarking,"** *IEEE Trans Electron Devices*, Vol. 54, pp. 3195–3205, December. 2007.

[18] CH. Wang, K. Ryu, A. Badmeav, N. Patil, A. Lin, S. Mitra, PH. Wong and CH. ZHou, **"Device study, chemical doping, and logic circuits based on transferred aligned single-walled carbon nanotubes,"** *Physics Letters*, Vol. 93,No. 3, pp. 033101 – 033101-3, July. 2008.

[19] S. University, CNFET model Website, Stanford, [Online]. Available at: http://nano.stanford.edu/model.php?id=23.

[20] D. Biolek, V. Biolkova, Z. Kolka, **"AC analysis of operational rectifiers via conventional circuit simulators,"***WSEAS Transactions on Circuits and Systems*, Vol. 3, No. 10, pp. 2291 – 2295, 2004.

[21] Liang, J., Chen, L., Han, J., Lombardi, *F.:* **Design and Evaluation of Multiple Valued Logic Gates using Pseudo N-type Carbon Nanotube FETs** *13(4), 695*-708 (2014).

[22] M. H. Moaiyeri, R. F. Mirzaee, A. Doostaregan, K. Navi, O. Hashemipour, "**A universal method for designing low-power carbon nanotube FET-based multiple-valued logic circuits**" *IET Computers & Digital Techniques*, Vol. 7, No**.** 4, pp. 167-181, 2013.

[23] S. L. Murotiya, A. Gupta, **"CNTFET-Based Design of Content-Addressable Memory cell**," *International Journal of Electronics Letters (2014)*, doi: 10.1080/21681824.2014.911368.

[24] S. A. Ebrahimi, P., Keshavarzian, **"Fast low-power full-adders based on bridge style minority function and multiplexer for nanoscale,"** *International Journal of Electronics*, Vol. 100, No. 6, pp. 727-745, 2013.

[25] K. Sridharan, S. Gurindagunta, and V. Pudi, **"Efficient multiternary digit Adder design in CNTFET technology,"** *Nanotechnology, IEEE Transactions* on, Vol. 12, No. 3, pp. 283-287, 2013.

[26] M. Jamalizadeh, F. Sharifi, M. H. Moaiyeri, K. Navi, O., Hashemipour, **"Five new MVL current mode differential absolute value circuits based on carbon nano-tube field effect transistors (CNTFETs),"** *Nano-Micro Letters*, Vol. 2, No. 4, pp. 227-234, 2011.

[27] P. Keshavarzian, K. Navi, **"Universal ternary logic circuit design through carbon nanotube technology,"** *International Journal of Nanotechnology*, Vol. 6, No. 10, pp. 942-953, 2009.

[28] S. Lin, Y. B. Kim, and Lombardi, **"Design of a ternary memory cell using CNTFETs,"** *Nanotechnology, IEEE Transactions on*, Vol. 11, No. 5, pp. 1019-1025, 2012.

[29] S. Lin,Y. B. Kim, and F. Lombardi, **"The CNTFET-based design of ternary logic gates and arithmetic circuits,"** *IEEE Trans. Nanotechnol*, Vol. 10, No. 2, pp. 217–225, 2011.

[30] A. Raychowdhury, K., Roy, **"Carbon-nanotube-based voltage-mode multiple-valued logic design,"** *Nanotechnology, IEEE Transactions* on, Vol. 4, No. 2, pp. 168-179, 2005.

[31] P. Keshavarzian, K. Navi, **"Efficient Carbon Nanotube Galois Field Circuit Design**", *IEICE Electronics Express*, Vol. 6, pp. 546–552, 2009.

[32] S. Lin, Y. B. Kim, and F. Lombardi, "**Design of a CNTFET-based SRAM Cell by Dualchirality Selection**", *IEEE Transactions on Nanotechnology*, Vol. 9, pp. 30–37, 2010.

[33] P. Keshavarzian, **"Novel and general carbon nanotube FET-based circuit designs to implement all of the 39 ternary functions without mathematical operations,"** *Microelectronics Journal*, Vol. 44, No. 9, pp. 794-801, 2013.

[34] Navi, Keivan, et al. "**Two novel ultra-high speed carbon nanotube Full-Adder cells**," *IEICE Electronics Express*, 6.19, pp. 1395-1401, 2009.

[35] Jamjaem, Theerayut, and Bancha Burapattanasiri. "**High Precision HalfWave Rectifier Circuit In Dual Phase Output Mode**," *arXiv preprint arXiv:1001.2253*, 2010.

[36] B., Boonchai, W. Surakampontom, "**A CMOS Current-mode squarer/rectifier circuit**," Circuits and Systems, 2003. ISCAS'03. *Proceedings of the 2003 International Symposium on*. Vol. 1, 2003.

[37] Ch. Ch. Chang, Sh.-I. Liu, **"Current-mode full-wave rectifier and vector summation circuit**," *Electronics Letters* 36.19, pp. 1599-1600, 2000.

[38] K., Jaroslav, N. Herencsar, and K. Vrba, **"Minimal configuration versatile precision full-wave rectifier using current conveyors**," *Proceedings of the European Conference of Circuits Techonology and Devices-ECCTD* 2010, 2010.

[39] Monpapassorn, Adisak, et al., **"CMOS High Frequency/Low Voltage Fult-Wave Rectifier,**" *Thammasat Int. J. Sc. Tech* 8.2, 2003.

[40] R., Vanchai, R. Guntapong, **"A low-voltage wide-band CMOS precision full-wave rectifier**" *International journal of electronics* 89.6, pp. 467-476, 2002.

[41] Ramirez-Angulo, J., et al. "**Very low-voltage class AB CMOS and bipolar precision current rectifiers**" *Electronics Letters* 35.22, pp. 1904-1905, 1999.

[42] Ramirez-Angulo, J. "**High frequency low voltage CMOS diode**" Electronics *Letters* 28.3, pp. 298-299, 1992.

[43] Ch. Ch. Chang, Sh.-I. Liu, **"Current-mode full-wave rectifier and vector summation circuit**" *Electronics*

Letters 36.19, pp. 1599-1600, 2000.

[44] W. Surakampontorn, R. Vanchai, **"Integrable CMOS sinusoidal frequency doubler and full-wave rectifier**" *International Journal of Electronics* 73.3, pp. 627-632, 1992.

[45] K., Jaroslav, N. Herencsar, and K. Vrba**, "Current-mode precision full-wave rectifier using single DXCCII and two diodes**" *Circuit Theory and Design (ECCTD), 2011 20th European Conference on. IEEE*, 2011.

[46] Kh. Surachet, V. Kasemsuwan, **"High performance CMOS current-mode precision full-wave rectifier (PFWR**)" *Circuits and Systems, 2003. ISCAS'03. Proceedings of the 2003 International Symposium on. Vol. 1. IEEE*, 2003.

[47] M. Adisak, K. Dejhan, and F. Cheevasuvit, **"CMOS dual output current mode half-wave rectifier**" *International Journal of Electronics* 88.10, pp. 1073-1084, 2001.